Ceramics-Silikáty 63 (2), 185-193 (2019)
www.ceramics-silikaty.cz doi: 10.13168/cs.2019.0010

THE EFFECT OF SEALING PROCESSES ON THE CORROSION BEHAVIOUR OF Al_2O_3-13 wt. % TiO_2 COATING

SHAO JIA*, #WANG ZEHUA*, SI LIQIONG**, ZHOU ZEHUA*, ZHANG XIN*, JIANG SHAOQUN*, WANG GANG*

*College of Mechanics and Materials, Hohai University, Nanjing, 211100, China
**Shanghai Aerospace Electronic Technology Institute, Shanghai 201109, China

#E-mail: zhwang@hhu.edu.cn

Submitted January 11, 2019; accepted February 17, 2019

Keywords: Ceramic Coating, Corrosion, Sealing, Protection, Ultrasonic excitation

A novel post-treatment process was employed to seal a plasma-sprayed Al_2O_3-13 wt. % TiO_2 (AT13) coating to improve its corrosion resistance. A series of AT13 coatings were sealed with silicone resin using conventional sealing and ultrasonic sealing at different temperatures. The effect of the sealing treatment on the corrosion behaviours of the coatings were investigated with salt spray tests and electrochemical methods. Most of the ultrasonic sealed coatings had less weight loss than conventional sealed coatings after the salt spray test. In 5.0 wt. % NaCl solutions, the ultrasonic sealed coating had the higher corrosion potential and the lower corrosion current density. The coating sealed at 40 °C has the lowest corrosion weight loss, lowest corrosion current densities and highest corrosion potential, compared with conventional sealed coating. It means that ultrasonic sealing can improve the corrosion resistance of plasma-sprayed AT13 coating effectively and the temperature was a key factor in the sealing treatment.

INTRODUCTION

From an economic point of view, steel is a kind of suitable material for many applications [1]. Manufacturing ceramic coatings with high wear-, corrosion-resistance is important for many industrial processing applications [2, 3]. As a mature technology, thermal spraying process has been widely used to deposit ceramic coatings on different metals, such as steels [4, 5, 6], irons [7], aluminium alloys [8], superalloys [9] to protect the substrate from wear [10, 11], corrosion [12], thermal fatigue [13] and cavitation erosion [14] for a long service life. Oxide ceramics, due to their excellent properties including high hardness, high chemical inertness [13, 14] in a variety of aggressive environments [15], and good wear resistance, are promising candidates as corrosion-resistant coatings in industrial applications, although there are some inevitable defects in the coatings [16, 17]. Generally, the defects come from unmelted particles, inadequate flow or fragmentation of molten particles under impact status, shadowing effects caused by an improper spraying angle, and entrapped gas [18]. Moreover, vertical and horizontal cracks or pores may occur due to the high cooling rate of the individual splats and poor inter-lamellar bonding [19]. Accordingly, these structural flaws result in not only a bad corrosion resistance of coating-substrate system but also poor mechanical properties as well as wear resistance of the coating [16]. Hence, a lot of attention has been paid to reduce the pores and cracks. Although the optimisation of the spraying parameters has brought a decrease in the porosity, it is hard to obtain a completely dense ceramic coating without any cracks [6], which means the transportation of corrosive medium to the substrate cannot be prevented still. Therefore, a number of post-treatments have been adopted to the plasma sprayed ceramic coating to reduce the pores and cracks, such as laser remelting, inorganic sealing treatment [16, 20, 21]. Laser remelting process can make it possible to obtain a perfectly cohesive coating; however, some micro-cracks may still exist in the coatings due to the thermal shrinking and rapid cooling rate [16, 22]. For the conventional sealing treatment, the sealant cannot always penetrate deeply into the coating through the open micro-pores and micro-cracks due to its surface tension and viscosity.

In this study, a novel sealing treatment with ultrasonic excitation is introduced, which can effectively decrease the porosity and improve the corrosion resistance of the coatings. Owing to the localised high temperature [23] and pressure caused by ultrasonic cavitation [24], the tiny bubbles collapse [25] and escape in those working areas. Meanwhile those activated bubbles could also enhance the fluidity of the sealant and interaction between the coatings and the sealant. So, the micro-pores and micro-cracks can also be sealed to a large extent by the sealant, while they are difficult to be sealed in conventional impregnating sealing treatments without ultrasonic excitation.

EXPERIMENTAL

Plasma sprayed NiCrAl/Al_2O_3-13 wt. % TiO_2 (AT13) coatings were deposited on mild steel with atmospheric plasma spray equipment (PRAXAIR-3710). The plasma spraying was carried out with the spraying parameters in Table 1. The thickness of the bond layer and the working layer were approximately 60 ~ 80 μm and 270 ~ 300 μm. All substrates were machined to the size of 24 × 24 × × 6 mm, and blasted before spraying to obtain a rough surface (Ra > 25 μm).

Before sealing, the coatings were ultrasonically cleaned and dried at 70 °C. A silicone resin having the properties shown in Table 2 was used as the sealant and the sealing treatment was performed with the method of soaking in the sealant. The coatings were sealed at 20, 40, 60, 80 °C respectively and impregnated in the sealant for 60 min under a field with a frequency of 40 kHz, as illustrated in Figure 1. The ultrasonic generator kept vertically to the sealing surface of coating. The sealed coating was dried in the air first for about 20 min and then cured at 115 °C in the oven for 15 min. After that, the coating surface with the residue of the sealant was ground using 1200#SiC grit to ensure that the ceramic surface of the coating was exposed in order to be tested.

The corrosion resistance of the AT13 coatings was evaluated using 5 wt. % NaCl solution spraying test at 35 °C. After each corrosion test, the samples were cleaned under running water, and then air-dried first for 30 min and then dried in an oven at 115 °C for 2 hours. An electron balance with a sensitivity of 10^{-4} g was used to measure the weight loss of the samples before and after the spraying test.

The electrochemical corrosion properties of the coating were performed using a PARSTAT 2273 Advanced Electrochemical System. A neutral solution containing 5.0 % NaCl in deionised water was used as the electrolyte. The electrode potential was raised from –250 to +250 mV with a rate of 1 mV·s^{-1}, and the current flowing through the coating-substrate system was recorded. Also, a calomel electrode was used as the reference electrode and a platinum one was used as the auxiliary electrode. In addition, the contact area in all the cases was 1 cm^2. A stabilisation period of 30 min was employed before the test.

For comparing, the corrosion performance of the as-sprayed coating and a conventional sealed coating were also investigated. The conventional sealing process was similar to the ultrasonic sealing process except that no ultrasonic was applied. The morphology of the corroded coating was observed under an OLMPUS-BX51M optical microscope (OM) and a HITACHI-3400N scanning electron microscope (SEM).

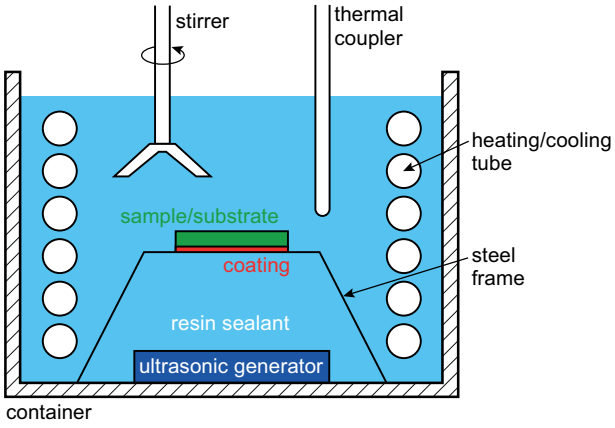

Figure 1. Schematic diagram of the sealing instrument for the coatings.

RESULTS

Salt spray tests

The cumulative weight losses of the coating in 5.0 wt. % NaCl salt spraying corrosion test are given in Figure 2. Generally, the as-sprayed coating had a greater weight loss than any sealed coating. It meant the sealed coatings had better anti-corrosion resistance than the as-sprayed coating. From Figure 2, it can be seen that at the first stage, both the as-sprayed coating and the ultrasonic sealed coating at 80 °C had a much higher weight losses than the other sealed coatings. After 30 days, the as-sprayed coating kept the highest cumulative weight loss still, but the cumulative weight loss of the sealed coating increased more slowly. Especially for the ultrasonic sealed coating at 80 °C, its cumulative weight

Table 1. Plasma spraying parameters.

Coating materials	Current (A)	Voltage (V)	Ar flow (l·min^{-1})	He flow (l·min^{-1})	Carrier gas (l·min^{-1})	Feed rate (g·min^{-1})	Spray distance (mm)	Moving speed (mm·s^{-1})
NiCrAl	700	40.5	56.6	24	7.5	26.8	100	150
AT13	900	39.5	42.5	27	7.5	44.2	100	80

Table 2. The properties of the silicone resin sealant.

pH	Viscosity (Pa·s; 25 ± 1 °C)	Density (g·cm^{-3}; 25 ± 1 °C)	Adhesive capacity	Dielectric strength (kV·mm^{-1})
6 – 7	9.7 - 14.0	0.87 – 0.95	1	30 – 50

loss was close to the conventional sealed coating. After the 72-day spraying test in 5 wt. % NaCl, the weight loss of conventional sealed coating was 65.2 % of the as-sprayed coating and the ultrasonic sealed coating at 40 °C had the lowest cumulative weight losses. Its cumulative weight loss was approximately 46.2 % of the conventional sealed coating, and 30.1 % of the as-sprayed coating. The different coating ranked in the sequence of the cumulative weight loss, from low to high, was the ultrasonic sealed coating at 40 °C, the ultrasonic sealed coating at 60 °C, the ultrasonic sealed coating at 20 °C, the conventional sealed coating, the ultrasonic sealed coating at 80 °C and the as-sprayed coating. So, it can be concluded that the sealing treatments with ultrasonic excitation could improve the anti-corrosion resistance of the plasma sprayed AT13 coating efficiently, and the sealing temperature had an effect on the corrosion resistance.

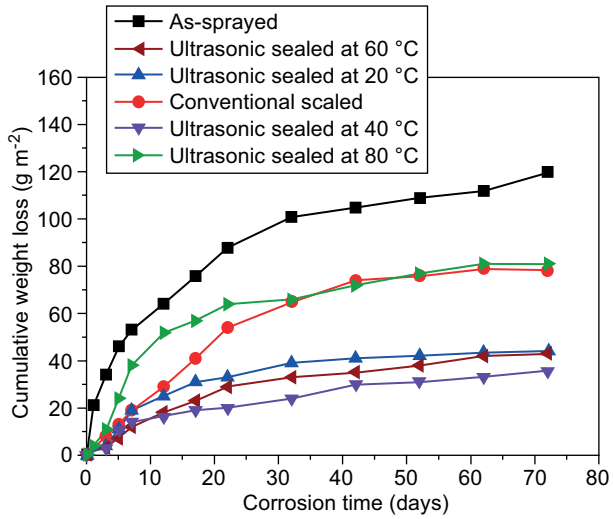

Figure 2. The cumulative weight losses of the coatings during the salt spraying test.

The surface images of the coating corroded for 72 days with 5 wt. % NaCl salt spraying test are given in Figure 3. A large number of cracks and flaking failures were observed in the as-sprayed coatings, as seen in Figure 3a-1, 3a-2. Some corrosion products and spots of failure were also found on the conventional sealed coating (Figures 3b-1, 3b-2) and the ultrasonic sealed coating at 80 °C (Figures 3f-1, 3f-2). No corrosion products and cracks were found on the surface of the ultrasonic sealed coating at 20 °C, 40 °C (Figure 3c,d).

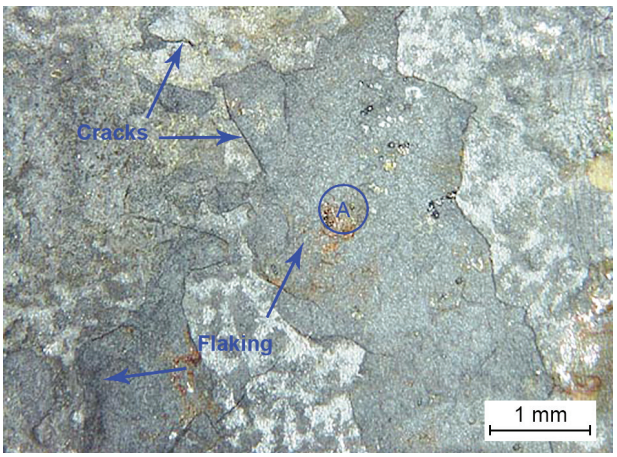

a-1)

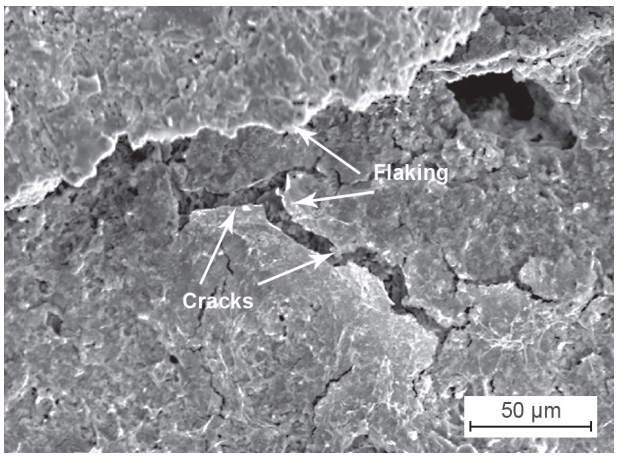

a-2)

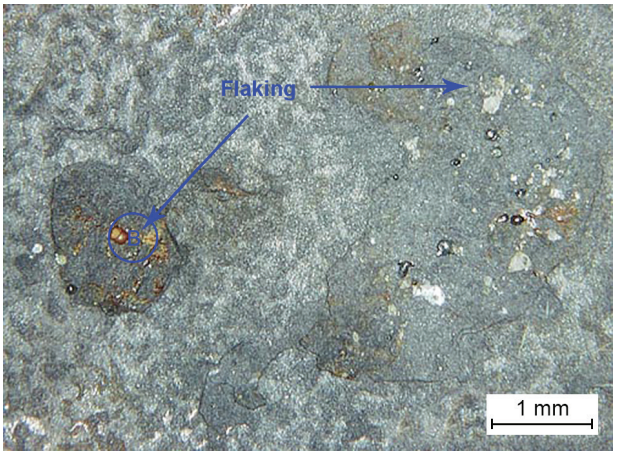

b-1)

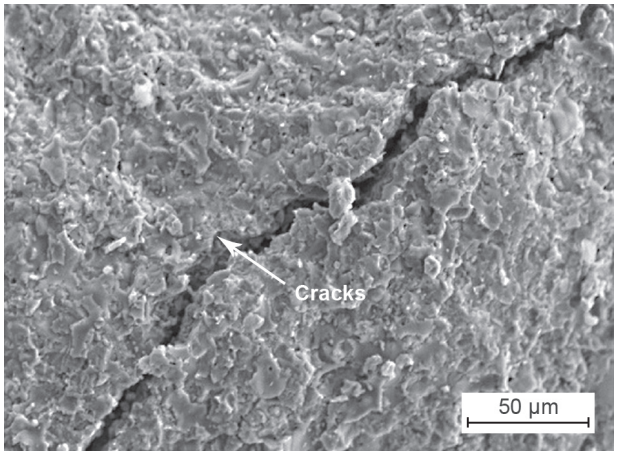

b-2)

Figure 3. Surface images of the coatings corroded in 5 wt. % NaCl salt spray for 72 days. *(Continue on next page)*

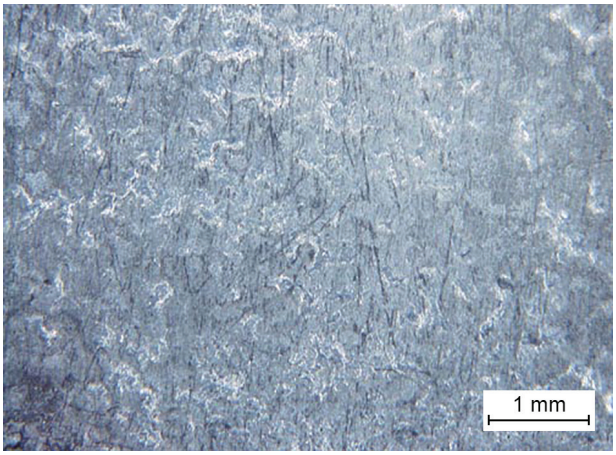

c)

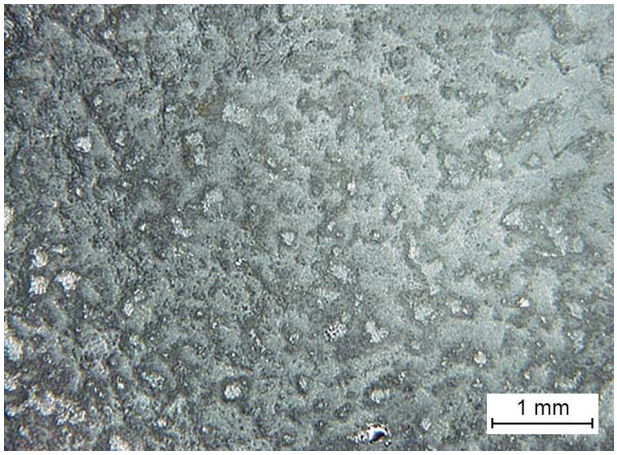

d)

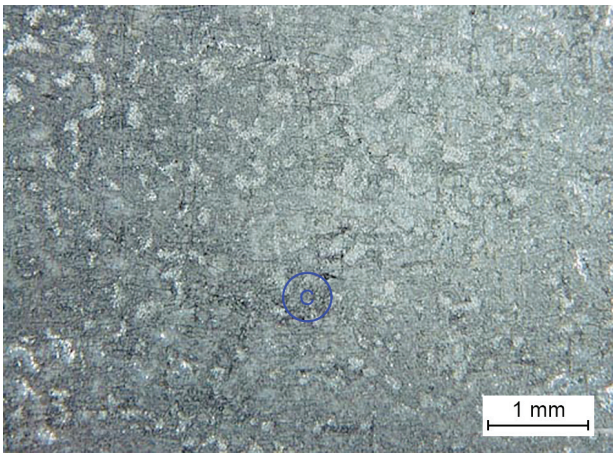

e-1)

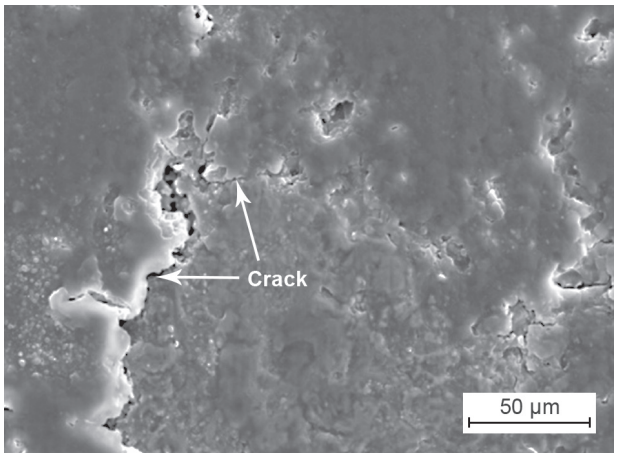

e-2)

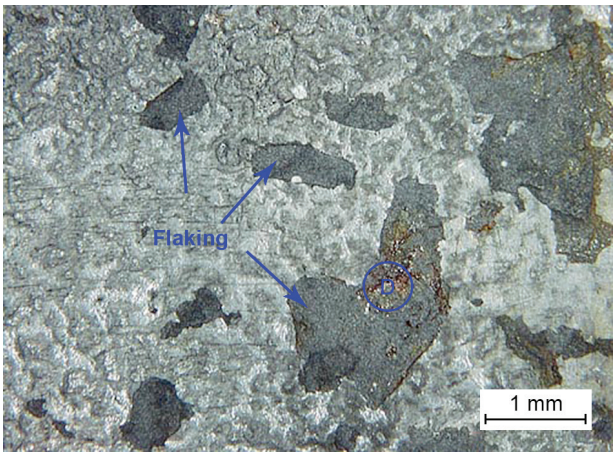

f-1)

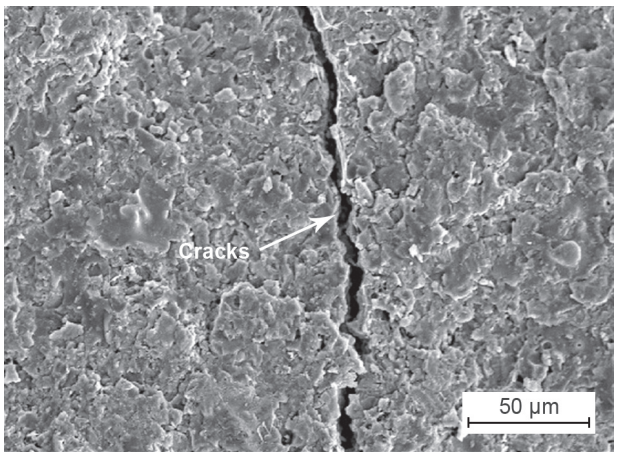

f-2)

Figure 3. Surface images of the coatings corroded in 5 wt. % NaCl salt spray for 72 days.

A yellow point, Area C, was found on the surface of the ultrasonically sealed coating at 60 °C, as shown in Figure 3e-1. Its SEM image is shown in Figure 3e-2. It can be seen that there were some micro-cracks on the corroded surface.

As shown in Figure 4a, it can be clearly seen that some partially and/or fully melted particles, structural flaws such as cracks and pores were distributed on the surface of the as-sprayed coating. The corrosive medium can penetrate the coating through the open pores and/or cracks to the substrate. Corrosion takes place at the boundary of the ceramic coating and the steel substrate and the volume expansion of its corrosion products will develop the inner stress and cracks. With the development of the corrosion, some areas of the coating would flake off unavoidably. From the test results, as

shown in Figures 3b-1, 3b-2 and 3f-1, 3f-2, it could be supposed that when the sealing process was used, the pores and cracks were sealed, as shown in Figure 4b. During the salt spray test, the sealant in the pores and cracks would gradually also be corroded. When the sealant in the pores and cracks was corroded off, the corrosion medium would pass through the ceramic coating to the pores and/or cracks to corrode the steel substrate and the result that some spots of the coating would flake off. For this reason, the deeper the sealant penetrates into the coating, the better the anti-resistance of the sealed coating.

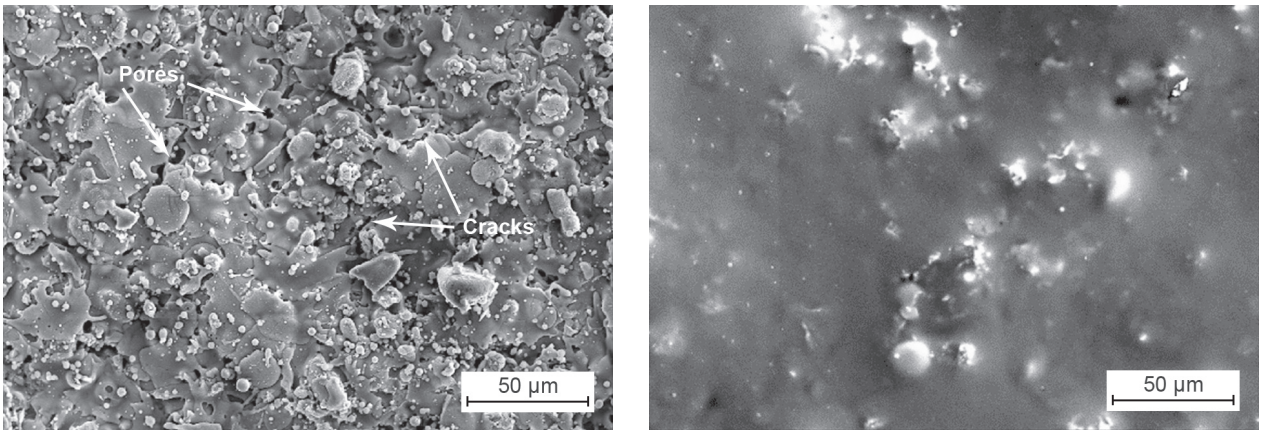

a) as-sprayed coating b) sealed coating

Figure 4. Surface images of the coatings before and after sealing: a) surface images of the as-sprayed coating; b) surface images of the sealed coating.

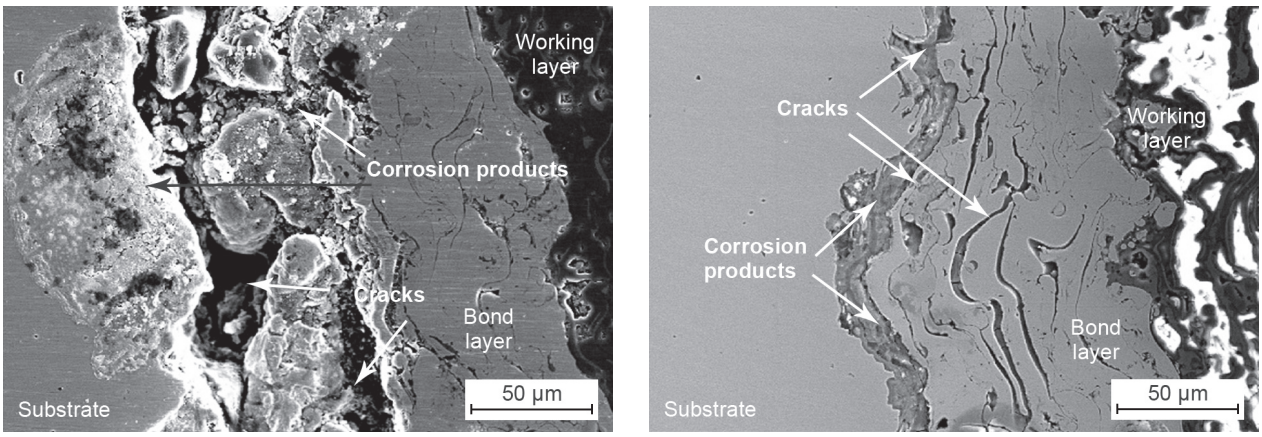

a) as-sprayed b) conventional sealed

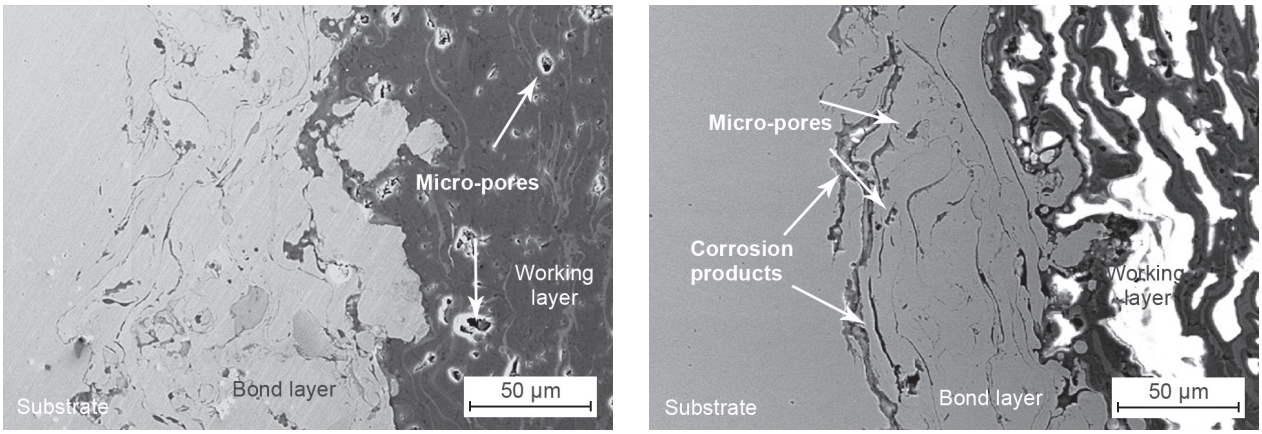

c) ultrasonic sealed at 60 °C d) ultrasonic sealed at 80 °C

Figure 5. Cross-section images of the coatings after the salt spray test for 72 days: a) the as-sprayed; b) the conventional sealed; c) the ultrasonic sealed at 60 °C; d) the ultrasonic sealed at 80 °C.

The typical cross-section images of the corroded coatings are given in Figure 5. A big crack and some corrosion products were observed on the interface between the substrate and as-sprayed coating, as shown in Figure 5a. The path of the cracks preferentially was seen clearly along the boundary of the coatings and the substrate. Some tiny corrosion products and micro-cracks were also found on the cross-section image of both the conventional sealed coating and the ultrasonic sealed coating at 80 °C (Figures 5b and 5d). However, as shown in Figure 5c, the corrosion phenomenon of the ultrasonic sealed sample at 40 °C was not obvious, and there were only some micro-pores in the working layer. From the typical cross-section images of the corroded coatings, it was concluded that ultrasonic sealing had a better effect to protect the plasma sprayed coating from the corrosion than the conventional sealing. Besides, the sealing temperature had an obvious effect on the sealing quality. The ultrasonic sealed coatings at 40 °C performed the best.

Electrochemical corrosion tests

The Tafel polarisation curves of the as-sprayed coatings, the conventional sealed coatings, the ultrasonic sealed coatings in the 5.0 wt. % NaCl solution are showed in Figure 6. Since the corrosion current density (I_{corr}) and the corrosion potential (E_{corr}) are two critical parameters, the corresponding corrosion potential (E_{corr}) and corrosion current densities (I_{corr}) are measured and listed in Table 3.

As well-known, a higher value of the corrosion current density and/or a more negative value of the corrosion potential would indicate that the coating-substrate system has less resistance to corrosion. From Table 3, it can be found that the substrate exhibited a lower corrosion resistance than any coating. Among all of the coatings, the as-sprayed coating had the lowest corrosion potential (E_{corr}) and the highest corrosion current densities (I_{corr}), which probably resulted from the fact that the corrosive medium immersed into the coating through the open pores and cracks. A high current density meant that the coating had a large volume of open porosity and, thus a high corrosion rate. The conventional sealed coating had a higher E_{corr} value (-0.562V) and a smaller I_{corr} value (0.495 μA·cm^{-2}) than the as-sprayed coating, which meant that conventional sealed coating had better anti-corrosion resistance than the as-sprayed coating. Among all of the ultrasonic sealed coatings, the coating sealed at 40 °C with ultrasonic excitation had the lowest I_{corr} value (0.125 μA·cm^{-2}), about 60 % of the as-sprayed coating; this test result was consistent with the findings during the spraying test that the ultrasonic sealed coating at 40 °C had the lowest cumulative weight losses, as seen in Figure 3. The coating sealed at 80 °C with the ultrasonic excitation had the lowest E_{corr} value (-0.468 V) and biggest I_{corr} value (0.634 μA·cm^{-2}). It meant that the ultrasonic sealed coating at 80 °C had the worst anti-corrosion properties among all the ultrasonic sealed coatings. This result reflected the fact that the sealing treatment can improve the anti-corrosion resistance of the plasma-sprayed AT13 coatings effectively. The sealing treatment with ultrasonic excitation can strengthen the sealing effectiveness of the coatings. From the test results of Table 2, it is not difficult to conclude that the proper temperature for the AT13 coating to be sealed under ultrasonic excitation should be 40 °C.

Figure 7 is the composite plot of the current densities and weight loss of the different coatings from the electrochemical corrosion tests and salt spray tests. It showed that the regulations of the weight loss of the different coatings had a good relationship with the current densities in the 5.0 wt. % NaCl solution. For the steel substrate, the as-sprayed coating and the conventional sealed coating, the current density and the weight loss decreased correspondingly. For the ultrasonic sealed coating, the current densities did not change too much, the weight losses changed a little except for the coating sealed at 80 °C, which had the biggest weight and current density among all of the ultrasonic sealed coatings, but its weight loss increased too quickly, compared with the increase of the current density.

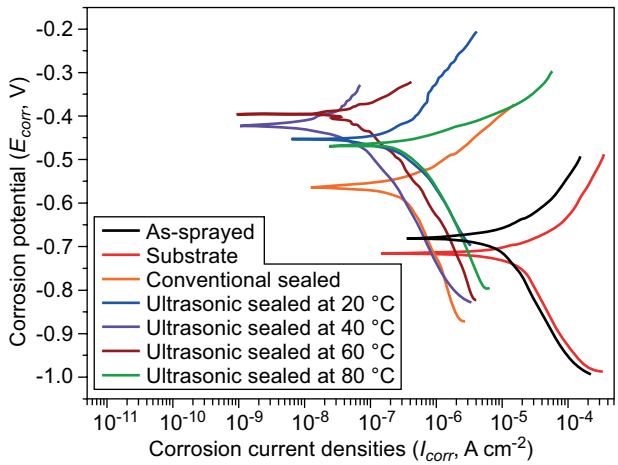

Figure 6. The Tafel polarisation curves of the steel substrate and the coatings.

Table 3. The corrosion current density (*Icorr*) and potentials (*Ecorr*) of the test coatings.

Sealing treatment	Corrosion potentials E_{corr} (V)	Corrosion current density I_{corr} (μA·cm^{-2})
Substrate	-0.715	28.65
As-sprayed	-0.679	20.74
Conventional sealed	-0.562	0.495
Ultrasonic sealed at 20 °C	-0.454	0.489
Ultrasonic sealed at 40 °C	-0.420	0.125
Ultrasonic sealed at 60 °C	-0.399	0.141
Ultrasonic sealed at 80 °C	-0.468	0.634

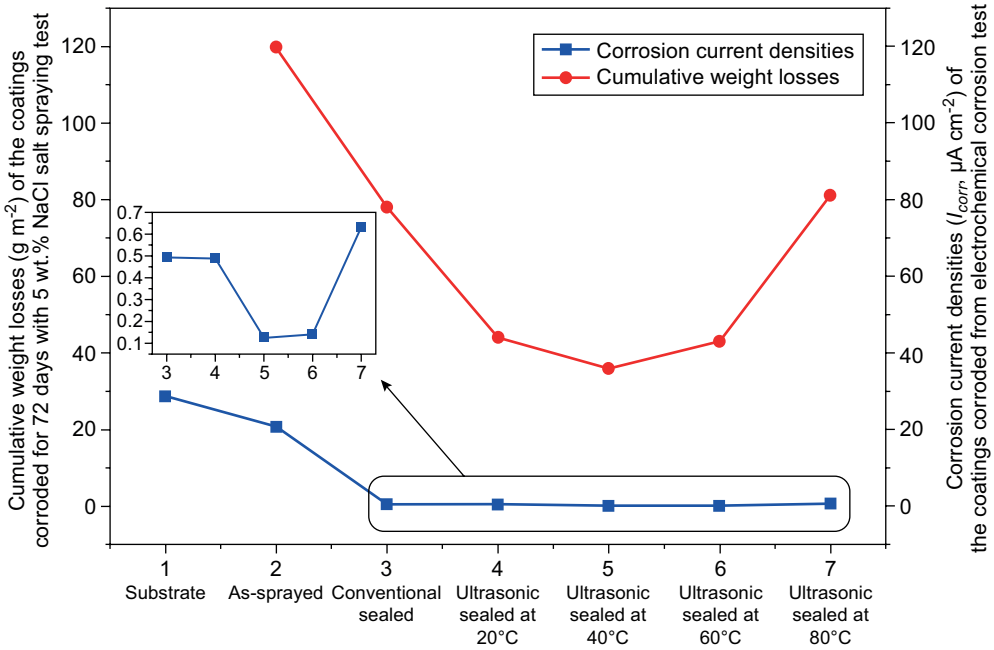

Figure 7. A composite plot of the current density and the weight loss of the substrate and the coatings.

DISCUSSION

As well-known, ceramics have excellent chemical stability. It should protect the steel substrate well from corrosion in a 5.0 wt. % NaCl solution. Unfortunately, there are certain micro-pores and micro-cracks in the as-sprayed ceramic coating due to the characteristic of the formation of the coating [17, 18, 26]. Some of the open pores and cracks will act as the tunnel for the corrosion medium to penetrate the coating to corrode the substrate. As was shown in Figures 3-7, the sealing treatment under ultrasonic excitation can greatly improve the anti-corrosion resistance of the coating. It could be considered due to the sealing effect of the process. The previous study revealed that the sealing treatment under an ultrasonic field could effectively decrease the porosity of the plasma sprayed AT13 ceramic coating [27]. More sealant was filled into the porosity through the open micro pores and cracks of the coating. As a result, more tunnels of the corrosion medium were blocked by the sealant and less corrosion will take place.

Ultrasonic excitation plays an important role in sealing treatments. It may be the ultrasonic cavitation effect first which produces a force at the interface between the coating and the sealant solution to push the sealant into the pores and cracks. Secondly, the ultrasonic excitation can accelerate the activation of the sealant resin and improve the wettability of the sealant to the ceramic coating. Meanwhile, the ultrasonic excitation can reduce the viscosity of the sealant due to the fact that the ultrasonic sealant produced a number of localised hot spots [23, 25]. Compared with conventional impregnating sealing, ultrasonic excitation sealing can seal more pores and cracks, even those micro-pores and micro-cracks which may not be sealed with a conventional sealing treatment. With the force produced by ultrasonic excitation, more sealant can be pushed deeper into the pores and cracks. As a result, the ultrasonic sealed coating has less cumulative weight losses during the salt spraying test (shown in Figure 2) and lower corrosion current densities and higher potentials (shown in Table 3).

In addition, the effect of the ultrasonic excitation on the sealing treatment was affected by the temperature. When increasing the sealing temperature from 20 °C to 60 °C, the porosity of the coating clearly decreased, and the corrosion resistance correspondingly increased. However, the corrosion resistance of the coatings cannot be further improved when the temperature is over 60 °C. The coating sealed at 80 °C with ultrasonic excitation had a lower corrosion resistance than the coating sealed at 40 °C to 60 °C with ultrasonic excitation, as shown in Figure 2 and Table 3. This is because the sealant solution is a liquid mixture based on alcohol with a low boiling point of 78.2 °C. When the sealing temperature is over 78.2 °C, the sealant solution begins to boil and a lot of bubbles are produced. Adsorbing them on the coating surface would produce a negative effect on the sealing treatment.

CONCLUSIONS

A novel post-treatment process was employed to seal a plasma-sprayed Al_2O_3-13 wt. % TiO_2 coating to improve its corrosion resistance. The effect of the

sealing treatment on the corrosion behaviours of the coatings were investigated with salt spray tests and electrochemical methods. The following conclusions can be drawn from this work:

- Comparing to the conventional sealing process, the ultrasonic excitation had a reinforced effect on the sealing treatment of AT13 coating. After 72 days of salt spray testing in 5.0 wt. % NaCl, the weight loss of the ultrasonic sealed coating at 40 °C was approximately 46.2 % of the conventional sealed coating, and 30.1 % of the as-sprayed coating.
- The ultrasonic sealing treatment could improve the electrochemical corrosion resistance of the Al_2O_3-13 wt. % TiO_2 coating in the 5.0 wt. % NaCl solution. The ultrasonic sealed coating at 40 °C had the lowest I_{corr} value of 0.125 $\mu A \cdot cm^{-2}$, much lower than the value of as-sprayed coating (20.74 $\mu A \cdot cm^{-2}$) and the value of conventional sealed coating (0.495 $\mu A \cdot cm^{-2}$).
- The temperature was a key factor during the sealing treatment when an organic resin was employed to seal the coating. The coating sealed at 40 °C has the lowest corrosion weight loss, lowest corrosion current densities (I_{corr}) and highest corrosion potential (E_{corr}).

REFERENCES

1. Parchoviansky M., Petrikova I., Barroso G. S., Svancarek P., Galuskova D., Motz G., Galusek D. (2018): Corrosion and oxidation behavior of polymer derived ceramic coatings with passive glass fillers on AISI 441 stainless steel. *Ceramics-Silikaty*, *2,* 146-157. doi: 10.13168/cs.2018.0006
2. Medvedovski E. (2012): Novel advanced ceramic and coating processing. *Advances in Applied Ceramics 111*, 243–245. doi: 10.1179/1743675312Z.00000000077
3. He B., Li F., Zhou H., Dai Y. B., Sun B. D. (2007): Microstructure and thermal cycling behavior of thermal barrier coating on near – α titanium alloy, *Journal of Coatings Technology & Research, 3*, 335-340. doi: 10.1007/s11998-007-9046-8
4. Momber A. W., Marquardt T. (2018): Protective coatings for offshore wind energy devices (OWEAs): a review, *Journal of Coatings Technology & Research, 1*, 13–40. doi: 10.1007/ s11998-01709979-5
5. Celik E., Ozdemir I., Avci E. (2005): Corrosion behaviour of plasma sprayed coatings. *Surface Coating & Technology, 193*, 297-302. doi: 10.1016/j.surfcoat.2004.08.143
6. Zhang N., Zhang N. N., Wei X. F., Zhang Y., Li D. Y. (2017): Microstructure and Tribological Performance of TiB_2-NiCr Composite Coating Deposited by APS. *Coatings, 7*, 238. doi: 10.3390/ coatings7120238
7. Ksiazek M., Boron L., Radecka M., Richert M., Tchorz A. (2016): The Structure and Bond Strength of Composite Carbide Coatings (WC-Co + Ni) Deposited on Ductile Cast Iron by Thermal Spraying. *Journal of Materials Engineering and Performance, 25*, 502-509. doi: 10.1007/ s11665- 015-1871-9
8. Naveena B. E., Keshavamurthy R., Sekhar N. (2017): Slurry erosive wear behaviour of plasma-sprayed fly ash–Al_2O_3 coatings. *Surface Engineering, 12*, 925-935. doi:10.1080/ 02670844.20170. 1288341
9. Doolabi M. S., Ghasemi B., Sadrnezhaad S. K., Habibolahzadeh A., Jafarzadeh K. (2018): Evaluation and Selection of Optimal Oxygen-Fuel Ratio for Best Mechanical Properties, Oxidation Resistance and Microstructure of HVOF NiCoCrAlY Coatings Using AHP–VIKOR Method. *Oxidation of Metals, 89*, 429–451. doi: 10.1007/s11085-017-9797-2
10. Yan J. H., He Z. Y., Wang Y., Qiu J. W., Wang Y. M. (2016): Microstructure and Wear Resistance of Plasma-Sprayed Molybdenum Coating Reinforced by $MoSi_2$ Particles, *Journal of Thermal Sprayed Technology, 7*, 1322-1329. doi: 10.1007/s11666-016-0440-6
11. Klyatskina E., Espinosa-Ferna´ndez L., Darut G., Segovia F., Salvador M. D., Montavon G. (2015): Agorges H., Sliding Wear Behavior of Al_2O_3–TiO_2 Coatings Fabricated by the Suspension Plasma Spraying Technique. *Tribology Letters, 8*, 1-9. doi: 10.1007/s11249-015-0530-5
12. Kim K. H., Kim J. H., Hong K. W., Park J. Y., Lee C. B. (2017): Application of high-temperature ceramic plasma-spray coatings for a reusable melting crucible, *Surface Coating & Technology, 362*, 429-435. doi: 10.1016/j. surfcoat.2017.02.010
13. Kumar D., Pandey K. N., Das D. K. (2016): Microstructure studies of air-plasma-spray-deposited CoNiCrAlY coatings before and after thermal cyclic loading for high-temperature application. *International Journal of Minerals Metallurgy and Materials, 8*, 934-942. doi: 10.1007/s12613 -016-1309-x
14. Jafarzadeh K., Valefi Z., Ghavidel B. (2010): The effect of plasma spray parameters on the cavitation erosion of Al_2O_3–TiO_2 coatings, *Surface Coating & Technology, 205*, 1850-1855. doi: 0.1016/ j.surfcoat.2010.08.044
15. Møller V. B., Dam-Johansen K., Frankær S. Kiil M., S. (2017): Acid-resistant organic coatings for the chemical industry: a review. *Journal of Coatings Technology & Research, 2*, 279–306. doi:10.1007/s11998-016- 9905-2
16. Knuuttila J., Sorsa P., Mäntylä T.(1999): Sealing of thermal spray coatings by impregnation. *Journal of Thermal Sprayed Technology, 2,* 249-257. doi:10.1007/s11666-999-0002-2
17. Hivart P., Crampon J. (2007): Interfacial indentation test and adhesive fracture characteristics of plasma sprayed cermet Cr_3C_2/Ni-Cr coatings. *Mechanics of Materials, 39*, 998-1005. doi:10.1016/j.mechmat. 2007.05.002
18. Zhang J. J., Wang Z. H., Lin P. H. (2013): Effects of sealing on corrosion behaviour of plasma-sprayed Cr_2O_3–$8TiO_2$ coating. *Surface Engineering, 8*, 594-599. doi: 10.1179/1743294413Y.0000000161
19. Kim H. J., Lee C. H., Kweon Y. G. (2001): The effects of sealing on the mechanical properties of the plasma-sprayed alumina-titania coating. *Surface Coating & Technology, 139*, 75-80. doi:10.1016/S0257 -8972(00)01132-4
20. Kim H. J., Odoul S., Lee C. H., Kweon Y. G. (2001): The electrical insulation behavior and sealing effects of plasma-sprayed alumina-titania coatings. *Surface Coating & Technology, 140*, 293-301. doi: 10.1016/S0257-8972(01) 01044-1
21. Jiao J., Luo Q., Wei X.S., Wang Y., Shen J. (2017): Influence of sealing treatment on the corrosion resistance of Fe-based. *Journal of Alloys and Compounds, 714*, 356-362. doi: 10.1016/j.jallcom.2017.04.179

22. Xie G., Lin X., Wang K., Mo X., Zhang D., Lin P. (2007): Corrosion Characteristics of Plasma-Sprayed Ni-Coated WC Coatings Comparison with Different Post-Treatment. *Corrosion Science, 49*, 662-671. doi: 10.1016/j.corsci.2006.04.016
23. Rae J., Ashokkumar M., Eulaerts O., Von Sonntag C., Reisse J., Grieser F. (2005): Estimation of ultrasound induced cavitation bubble temperatures in aqueous solutions. *Ultrasonics Sonochemistry, 12*, 325-329. doi: 10.1016/j.ultsonch.2004.06.007
24. Crum L. A. (1995): Comments on the evolving field of sonochemistry by a cavitation physicist. *Ultrasonics Sonochemistry, 2*, 147-152. doi:10.1016/1350-4177(95)00018-2
25. Iida Y., Yasui K., Tuziuti T., Sivakumar M. (2005): Sonochemistry and its dosimetry. *Microchemical Journal,. 80*, 159-164. doi: 10.1016/j.microc.2004.07.016
26. Zhang J. J., Wang Z. H., Lin P. H. , Lu W. H., Zhou Z. H., Jiang S. Q. (2011): Effect of Sealing Treatment on Corrosion Resistance of Plasma-Sprayed NiCrAl/Cr_2O_3-8wt.%TiO_2 Coating. *Journal of Thermal Sprayed Technology, 3*, 508-513. doi: 10.1007/s11666-010-9528-6
27. Si L. Q., Wang Z. H., Zhou Z.H. (2012): Influence of Sealing Treatments with Ultrasonic Excitation on Corrosion Resistance of Plasma-sprayed Al_2O_3-13wt%TiO_2 Coatings. *Rare Metal Materials and Engineering, 41*, 223-227. doi: 10.1016/j.mssp.2011.05.010